Ultrasharp edge filtering in nanotethered photonic wires

Anne Talneau, Isabelle Sagnes, R. Gabet, Yves Jaouën, Henri Benisty

Ultrasharp edge filtering in nanotethered photonic wires

A. Talneau, I. Sagnes, R. Gabet, Y. Jaouen, and H. Benisty

Citation: Appl. Phys. Lett. **97**, 191115 (2010); doi: 10.1063/1.3513279
View online: http://dx.doi.org/10.1063/1.3513279
View Table of Contents: http://apl.aip.org/resource/1/APPLAB/v97/i19
Published by the American Institute of Physics.

Ultrasharp edge filtering in nanotethered photonic wires

A. Talneau,[1,a)] I. Sagnes,[1] R. Gabet,[2] Y. Jaouen,[2] and H. Benisty[3]
[1]*Laboratoire de Photonique et de Nanostructures, CNRS, F-91460 Marcoussis, France*
[2]*Telecom ParisTech, F-75013 Paris, France*
[3]*Laboratoire Charles Fabry de l'Institut d'Optique, CNRS, Université Paris-Sud, F-91127 Palaiseau Cedex, France*

(Received 20 July 2010; accepted 18 October 2010; published online 12 November 2010)

Within a suspended photonic wire, the periodically-spaced nanotethers sustaining the wire can behave as damped transverse resonators that interact with the partially reflecting effect of the wire-tether intersection, and thus modify the Bragg reflection mechanism. This specific resonant mechanism is explored using a transfer matrix model, and is shown to result in an ultrasharp filter edge. This sharp behavior is evidenced experimentally on 300–400-nm-wide InP suspended wires through transmission data and further consolidated by optical low coherence reflectometry time-frequency analysis. © *2010 American Institute of Physics*. [doi:10.1063/1.3513279]

Optical filtering is a key function in all-optical networks. Simultaneously to a large rejection—at least 20 dB—the sharpest band edge is desired for a very selective spectral response. Such a sharp-edge reflector can also be of interest in optical modulation or switches. Ring-resonator-based filters have been extensively investigated: custom-designed filter shape can be obtained implementing a large number of coupled ring resonators.[1,2] A very sharp edge filter has also been theoretically proposed in a photonic crystal (PhC) environment, including phase-shift elements aside the PhC waveguide.[3] Both designs rely upon accurately designed coupled resonators.

A distinct resonant mechanism was proposed by Fan[4] to sharpen the resonant response of a side-coupled cavity by including it between weak reflecting elements, yielding an asymmetric shape and a much steeper edge. We demonstrate here that a periodic extrapolation of such a mechanism is responsible for the very sharp edge filtering that we measure on the Bragg stop-bands of nanotethered wires, in spite of the large radiation damping of the side-coupled resonators formed by the tethers. We first calculate using a transfer-matrix-model the spectral behavior of Bragg stop-bands in the direct periodic extrapolation of Ref. 4, and then modify it to qualitatively reproduce the periodic nanotethered wire geometry, the reflectors being the tether-wire intersections and the resonators being the nanotethers themselves. We further measure, using optical low coherence reflectometry (OLCR), a clearly longer delay for the stop-band associated with the sharper edge in transmission.

A photonic waveguide including a periodic perturbation of the dielectric constant exhibits a transmission stop-band (forbidden frequency range) due to the multiple in-phase feedback contributions, the well-known distributed Bragg reflector (DBR) effect. The stop-band width is determined by the feedback strength, and the stop-band edge sharpness is determined by the overall grating size (or its phase and amplitude distribution if it is variable). On this basis, addition of dissipative elements damps the filter shape while, on the contrary, reactive elements sharpen it.

In our case, the photonic wire is suspended in air through regularly spaced nanotethers [Fig. 1(a)]. The intersection can be considered as a reflector on the wire, while the tethers themselves can be considered as lossy resonators with partial reflection at their two ends due to the dielectric mismatch. When wires are relatively wide ($w=0.8$ to 0.6 μm), the nanotethers have been shown to operate mainly as a DBR, at a high order due to the large spacing/wavelength ratio (spacing $s=1$ to 10 μm).[5] When considering a narrower wire [$w=0.3$–0.4 μm, Fig. 1(b)], the side-coupling to the tethers becomes larger. We elucidate the positive role of the reactive (resonant) contribution of the tethers based on an extrapolation of Ref. 4, where the interplay of side-resonance and reflection to attain sharper edges was clarified.

We first consider the basic periodic extrapolation of Ref. 4 [Fig. 2(a)], with cavities centered between weak DBR individual elements, here simply modeled by a reflectivity $r=0.05$. The 2×2 transmission matrix product of a system essentially reads $(M_R M_\phi M_c M_\phi)^N$, where N is the number of periods and the four matrices account for reflection (M_R), cavity coupling (M_c), and the two identical phase sections M_ϕ, parametrized by the half-period phase $\phi=n_{eff}(\pi/\lambda)(s+t)$. The result for $N=100$ and $\gamma=0.0014$ (notation of Ref. 4), plotted in Fig. 2(b) as a transmission map versus 1/(normalized frequency) and normalized period $2(t+s)/n_{eff}\lambda$, is seen to be a staggered alternation of "enhanced DBR" and "inhibited DBR" stop-bands located across the deep resonator notch frequency. The DBR stop-bands would be of nearly constant depth without the resonator. Here, we

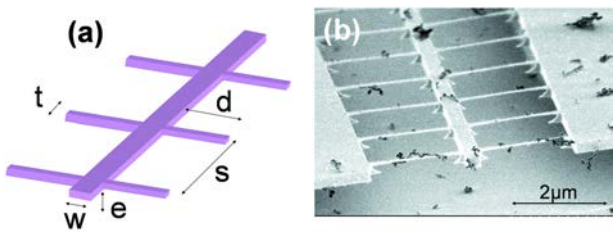

FIG. 1. (Color online) (a) Schematic of the tethered wire. (b) Scanning electron microscope picture of a suspended wire (spacing $s=2$ μm, tether length $d=2$ μm, wire width $w=0.3$ μm, tether width $t=70$ nm, and membrane thickness $e=260$ nm).

a)Author to whom correspondence should be addressed. Electronic mail: anne.talneau@lpn.cnrs.fr.

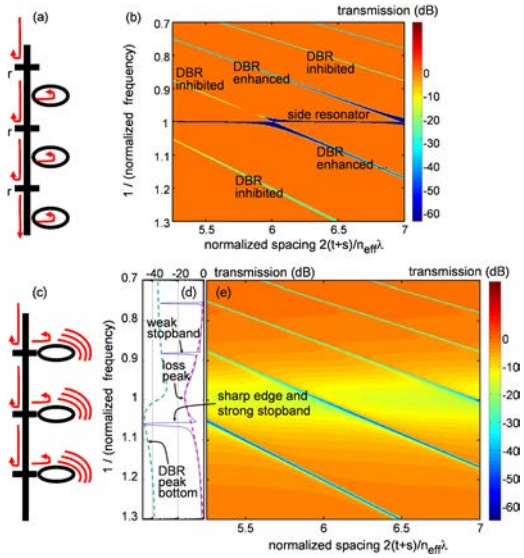

FIG. 2. (Color online) (a) Periodical reflector-resonator system; (b) transmission map (dB) with 1/(normalized frequency) axis centered on ω_o; (c) resonators now lie at the reflector locations and have large radiation losses; (d) transmission spectrum at the leftmost frequency of transmission map. (e) Dashed lines of (d) are explained in the figure.

focus on the DBR stop-band, we do not comment the sharpening of the deep resonator notch, noting that fundamentally both reactive phenomena interact and may potentially produce sharper features for any of them. The alternation obtained is a natural consequence of a standing wave pattern between reflectors, switching from node to antinode field at the center position of the cavities, that is, a switch for a step of 2π in the 4ϕ round-trip phase (hence $\Delta\phi=\pi/2$).

We further extrapolate a model more suited to the nanotethered wire case by localizing the side-resonators with the reflectors, see Fig. 2(c), hence by using now a transmission matrix product $(M_c M_R M_\phi M_\phi)^N$ still with r=0.05. We also add large losses in M_c since the featureless tethers are expected to be poor stublike resonators. The resonant terms in M_c now read $(\gamma/[\omega-\omega_o+i\gamma'])$ with a large γ' value, $\gamma'/\omega_o=0.08$, whereas $\gamma/\omega_o=0.0014$. We then observe [Figs. 2(d) and 2(e), plot and map] that in addition to the broad dip due to radiation losses centered at ω_o, there is a strong asymmetry of DBR stop-band strength between either sides of this dip.

Furthermore, the stop-band nearest to the dip acquires the desirable sharp edge on its short wavelength side. The overall behavior of stop-band strength is dictated by the real-part of the resonant term, $\mathrm{Re}(\gamma/[\omega-\omega_o+i\gamma'])$, manifesting its "reactive" origin ; therefore the tails of this effect scale with the slow decay $(\omega-\omega_o)^{-1}$ instead of the Lorentzian decay $(\omega-\omega_o)^{-2}$ of the central dip around $\omega=\omega_o$.

Suspended tethered wires were fabricated on a 260 nm thin suspended InP membrane. An established process based on ICP (Inductively Coupled Plasma) etching of nanopatterns followed by a selective etching of the sacrificial layer and a supercritical drying is used,[5,6] see Fig. 1(b). The following parameters were investigated: wire width $w=0.3$ to 0.8 μm, tether spacing $s=1$ or 2 μm, tether length $d=1$ to 2 μm, and tether width $t=70$ or 90 nm.

Transmission measurements are performed on 680-μm-long photonic wires, on an end-fire fiber set-up including a polarization-maintaining tuneable source in TM-like polarization (electric field E is vertical). In Fig. 3, the spectrally resolved transmission is plotted in the case of $w=0.4$ μm, $s=2$ μm, $d=2$ μm, and $t=70$ nm. We observe two resonances spaced by 146 nm, which corresponds to the free spectral range at $\lambda=1510$ nm for a cavity size $s=2$ μm, in agreement with the group index $n_g\approx 4$ calculated in Ref. 7. We clearly observe that the resonance at 1450 nm is shallow, while the one at 1590 nm exhibits a very sharp edge: the transmission drops by 25 dB on a 3 nm span. The 10 dB smoother trough at 1560 nm is attributed to a damped tether resonance, as introduced in the model. The shallow resonance lies far on the left of this trough while the sharp one is the resonantly enhanced one, in agreement with the calculated mechanism.

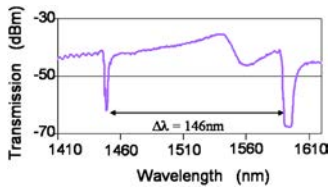

FIG. 3. (Color online) Experimental transmission for the tethered wire featuring $e=260$ nm, $s=2$ μm, $d=2$ μm, $t=70$ nm, and $w=0.4$ μm.

These resonances have been analyzed by OLCR, a powerful technique implemented to investigate slow light modes in PhC waveguides.[8] The same numerical algorithm exploiting the phase sensitive reflectogram in the spectral domain has been used; a 2 nm bandwidth sweeping filter is applied to produce the time–wavelength reflection maps plotted in Fig. 4. The OLCR source has a spectral range limited to 80 nm, which prevents both resonances of Fig. 3 to be observed simultaneously. In order to compare this coupled resonance to a classical Bragg resonance, we chose a wide wire ($w=0.8$ μm) where the coupled resonant sharpening effect disappears and we selected the Bragg resonance occurring in the OLCR spectral range. On Fig. 4(b), the classical Bragg effect produces a small and shallow resonance, the rear facet is visible, and a double-round trip is also visible with no increased delay. In the case of the "enhanced Bragg" effect

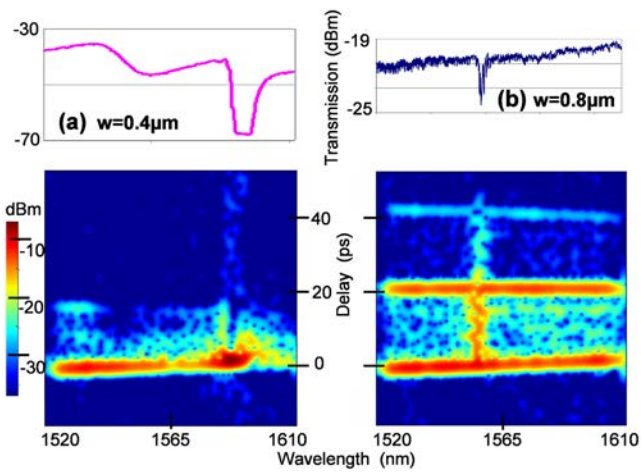

FIG. 4. (Color online) Time-wavelength reflection map for (a) a narrow wire w=0.4 μm exhibiting a sharp 25 dB drop (top inset), and for (b) a wide wire w=0.8 μm with classical Bragg filtering (3 dB drop, top inset). The slight slope of the front facet is due to the uncompensated dispersion of one arm of the interferometer. The larger delay of the rear facet reflection in (b) reflects the larger group index.

[Fig. 4(a)], the time delay is largely increased, which evidences the fact that the strongly enhanced feedback is "assisted" by the side resonators, with a longer energy storage. This is opposite to the trend of a stronger classical Bragg reflector, in which the smaller penetration would translate into a shorter delay.

The longer tether resonators ($d=2$ μm) exhibit the steepest filtering since they support a higher order mode of larger Q factor. For broader ($t=90$ nm) or shorter ($d=1$ μm) tethers, the coupled resonant mechanism is not observed since these geometries correspond to resonators of lower Q factor. For larger tether spacing ($s>2$ μm), the structure becomes too fragile and breaks. Higher Q resonators should lead to sharper filters with the same DBR bandwidth.

We have experimentally evidenced within a photonic wire held by regularly spaced thin nanotethers (70 nm) a coupled resonant mechanism leading to very sharp spectral filtering. The resonance takes place in each tether much like in a stub, and all resonators are coupled through the waveguide wire. The measured behavior can be understood by using a transfer matrix simulation that generalizes the approach of Fan.[4]

[1]D. G. Rabus, M. Hamacher, U. Troppenz, and H. Heidrich, IEEE J. Sel. Top. Quantum Electron. **8**, 1405 (2002).
[2]B. E. Little, S. T. Chu, P. P. Absil, J. V. Hryniewicz, F. G. Johnson, F. Seiferth, D. Gill, V. Van, O. King, and M. Trakalo, IEEE Photonics Technol. Lett. **16**, 2263 (2004).
[3]C. Chen, X. Li, H. Li, K. Xu, J. Wu, and J. Lin, Opt. Express **15**, 11278 (2007).
[4]S. Fan, Appl. Phys. Lett. **80**, 908 (2002).
[5]A. Talneau, K.-H. Lee, and I. Sagnes, IEEE Photonics Technol. Lett. **21**, 775 (2009).
[6]A. Talneau, K.-H. Lee, S. Guilet, and I. Sagnes, Appl. Phys. Lett. **92**, 061105 (2008).
[7]B. A. Daniel and G. P. Agrawal, Opt. Lett. **35**, 190 (2010).
[8]A. Parini, P. Hamel, A. De Rossi, S. Combrié, N.-V.-Q. Tran, Y. Gottesman, R. Gabet, A. Talneau, Y. Jaouën, and G. Vadalà, J. Lightwave Technol. **26**, 3794 (2008).